



19th Portuguese Conference on Pattern Recognition

**Instituto Superior Técnico, Lisboa
November 1st, 2013**



Programme Overview

Time	Event	Location
09h30 – 10h15	Registration	Salão Nobre, Pavilhão Central
10h00 – 10h15	Welcome session	Salão Nobre, Pavilhão Central
10h15 – 11h00	Poster session 1	Salão Nobre, Pavilhão Central
10h45 – 11h15	Coffee break	Salão Nobre, Pavilhão Central
11h15 – 12:00	Poster session 2	Salão Nobre, Pavilhão Central
12h00 – 14h00	Lunch break	Restaurante Café Império
14h00 – 15h30	Invited Talk by Prof. Ana Fred	Salão Nobre, Pavilhão Central
15h30 – 15h45	Coffee break	Salão Nobre, Pavilhão Central
15h45 – 16h45	Poster session 3	Salão Nobre, Pavilhão Central
16h45 – 17h00	Best poster award and closing session	Salão Nobre, Pavilhão Central

Invited Talk

Physiological Computing: a PR Perspective

Prof. Ana L. N. Fred

Department of Electrical and Computer Engineering, Instituto Superior Técnico, Lisbon and Instituto de Telecomunicações (IT), Lisbon.

Abstract:

In a sentence, physiological computing (PC) deals with the study and development of interactive systems that sense and react to the human body. The most basic sort of PC simply records a signal, such as a heartbeat, and displays it on a screen. More complex systems work on a basis of a bio-cybernetic loop, the main purpose of this loop being to translate patterns of physiological activity into meaningful interaction. From emotional status to identity assessment, this talk addresses the exploration of electrophysiological data in the context of intelligent human-computer interaction. Electrocardiographic signals and electro-dermal responses, acquired in a pervasive manner at the hands level, are shown to be two complementary modalities in the emotion / identity dual assessment goal. The role of pattern recognition in the development of such systems is discussed. Finally, BITalino, a versatile and low cost biosignal acquisition system is presented as a promising tool for pervasive biosignal monitoring and physiological computation.

Speaker Biography:



Ana Fred received the M.S. and Ph.D. degrees in Electrical and Computer Engineering, in 1989 and 1994, respectively, both from Instituto Superior Técnico (IST), Technical University of Lisbon, Portugal. She is a Faculty Member of IST since 1986, where she is currently a professor with the Department of Electrical and Computer Engineering. She is a researcher at the Pattern and Image Analysis Group of the Instituto de Telecomunicações. Her main research areas are on pattern recognition, both structural and statistical approaches, with application to data mining, learning systems, behavioral biometrics, and biomedical applications. She has done pioneering work on clustering, namely on cluster ensemble approaches. Recent work on biosensors hardware (including BITalino – www.bitalino.com) and ECG-based biometrics (Vitalidi project) have been object of several national and international awards, as well as wide dissemination on international media, constituting a success story of knowledge transfer from research to market. She has published over 160 papers in international refereed conferences, peer reviewed journals, and book chapters. She received the "Best paper award in Pattern Recognition and Basic Technologies", awarded by the IAPR, for the paper "Learning pairwise similarity for data clustering". She is the editor of over 40 books with the proceedings of international workshops that she organized or co-chaired, including S+SSPR 2004 (Lisbon), S+SSPR 2006 (Hong Kong), ICAART, KDIR and BIOSTEC and editor of 12 Springer books of selected papers.

Poster Session 1 (10h15 to 11h00)

- 1 **Staffline Detection in Grayscale Domain**
Ana Rebelo and Jaime Cardoso
- 2 **Cancer cell tracking using a Kalman filter**
Tiago Esteves, Maria Oliveira and Pedro Quelhas
- 3 **Automatic images spectral unmixing of Leishmania infection macrophage cell culture for improved infection indexes acessing**
Pedro Leal and Pedro Quelhas
- 5 **Mass detection on mammogram images: A first assessment of deep learning techniques**
Inês Domingues and Jaime Cardoso
- 6 **An Automatic Method for Assessing Retinal Vessel Width Changes**
Behdad Dashtbozorg, A. M. Mendonça and A. Campilho
- 14 **Learning from uneven video streams in a multi-camera scenario**
Samaneh Khoshrou, Jaime S. Cardoso and Luís F. Teixeira
- 17 **Land and water segmentation of SAR images using textons**
Francisco Seixas, Margarida Silveira and Sandra Heleno
- 20 **Quality measures for iris images in mobile applications**
Ana Sequeira, Juliano Murari and Jaime S. Cardoso
- 33 **Interactive Air Traffic Control automation in oceanic airspace**
Francisco Freitas, Rodrigo Ventura and Miguel Barão
- 38 **Large Scale Automatic Detection of Sub-km Craters Using Texture Information**
Marlene Machado, Lourenço Bandeira, Jorge Salvador Marques and Pedro Pina
- 39 **An interactive application for the detection of impact craters in planetary images**
Nuno Benavente, Lourenço Bandeira, Marlene Machado, José Saraiva, Jorge S. Marques and Pedro Pina
- 41 **3D Texture Analysis using Local Binary Patterns**
Pedro M. Morgado, Margarida Silveira and Jorge S. Marques
- 44 **3D Breast Parametric Model for Surgery Planning - a Technical Review**
Hooshar Zolfagharnasab, Jaime S. Cardoso and Helder P. Oliveira
- 45 **Total Variation Denoising using a Recursive and Spatially Adaptive Filter**
Manya Afonso and João Sanches
- 46 **Selection of epilepsy-related EEG ICA components for simultaneous fMRI analysis**
Rodolfo Abreu, Alberto Leal and Patrícia Figueiredo
- 53 **Clustering 802.11 Wireless Access Points Using Mixture of Hidden Markov Models**
Anisa Allahdadi, Ricardo Morla and Jaime S. Cardoso
- 55 **Towards efficient path planning of a mobile robot in rough terrain**
Diogo Amorim and Rodrigo Ventura
- 65 **Assessment of reliability of cerebrovascular reactivity measurements using breath-holding fMRI**
Joana Pinto, Inês Sousa, Pedro Vilela and Patrícia Figueiredo
- 66 **A Critical Analysis about a Motion-based Approach to Extract Global Trajectories**
Eduardo Marques, Jaime Cardoso and Ricardo Morla
- 67 **Ground-plane based indoor mobile robot localization using RGB-D sensor**
Miguel Vaz and Rodrigo Ventura
- 68 **Parameter Estimation for a Quad Rotor Dynamics**
Rui Oliveira and Rodrigo Ventura
- 70 **Exploring monogenic decomposition in carotid atherosclerotic plaque characterization**
David Afonso and João Sanches
- 72 **Sialolith metrics computed from microtomography data**
Pedro Nolasco, Antonio P. Alves de Matos, Paulo V. Coelho, Carla Coelho, António Máuricio, Manuel F.C. Pereira, Raúl C. Martins, João M.R. Sanches and Patricia A. Carvalho
- 73 **Automatic gesture segmentation based on a predictive event segmentation approach**
Sofija Spasojevic and Rodrigo Ventura

Poster Session 2 (11h15 to 12h00)

- 4 **An assessment of the potential of distinct facial regions for biometric recognition**
João C. Monteiro and Eduardo Mota
- 7 **Colour Invariant Features for Narrow-Band Imaging in Gastroenterological Examinations**
Bruno Mendes, Ricardo Sousa, Carla Rosa and Miguel Coimbra
- 8 **Insights into primates genomic evolution using a compression distance**
Diogo Pratas and Armando Pinho
- 11 **Impact of SVM Multiclass Decomposition Rules for Recognition of Cancer in Gastroenterology Images**
Ricardo Sousa, Mario-Dinis Ribeiro, Pedro Pimentel-Nunes and Miguel Tavares Coimbra
- 13 **Forecasting the Usage of Home Appliances with Denoised Signal Patterns**
Marisa Figueiredo, Bernardete Ribeiro and Ana Maria De Almeida
- 15 **Temporal subsampling impact on echocardiography based analysis of the left ventricle dynamics**
Susana Brás, José Ribeiro, Augusto Silva and José L. Oliveira
- 19 **Nociception/Anti-Nociception Balance During Anesthesia**
Ana Castro, Pedro Amorim and Miguel T. Coimbra

- 22 **Automatic Classification of Meals with Calorie Count**
Pedro Rodrigues, Pedro Brandão and Miguel Coimbra
- 23 **Face Recognition with Neural Networks Classifier using SIFT and SURF Descriptors**
João Sargo, João Caldas Pinto and João Costa Sousa
- 24 **Automatic Visual Inspection of Ceramic Plates based on SIFT and SURF Descriptors**
João Caldas Pinto, Rafael Baeta, Mariana Pereira, Ricardo Laranjeira, João Sargo and Carlos Cardeira
- 25 **Classificação da posição de estores de uma fachada de um edifício por análise de fotografias**
José Mota and João Caldas Pinto
- 26 **Building and Evaluation of a Mosaic of Images using Aerial Photographs**
João Costa, Tiago Coito, João Caldas Pinto and José Azinheira
- 34 **Development of a System for Automatic Detection of Air Embolism Using a Precordial Doppler**
Ana Rita Costa Tedim, Pedro Amorim and Ana Castro
- 35 **Neural Network Model for Wind Power Forecasting**
Paulo Salgado and Paulo Afonso
- 36 **Prediction of solar radiation using artificial neural networks**
João Faceira and Paulo Salgado
- 47 **Detection, classification and localisation of football players and ball from Handycam videos**
Tiago Vilas, J.M.F Rodrigues and Pedro Cardoso
- 50 **Region clustering using colour tuned keypoints**
Miguel Farrajota, J.M.F. Rodrigues and J.M.H. Du Buf
- 51 **AAM Based Vocal Tract Segmentation from Real-Time MRI Image Sequences**
Samuel Silva and António Teixeira
- 54 **Antifungal defensin Psd1 increases membrane roughness and promotes apoptosis in Candida albicans**
Patricia Silva, Sónia Gonçalves, Luciano Medeiros, Eleonora Kurtenbach and Nuno C. Santos
- 57 **Processing sports acquired information from a tracking system**
António Belguinha, Pedro Cardoso and J. M. F. Rodrigues
- 59 **Caracterização de Patologias da Pele por Ultrassons**
Sara Barbosa, Jose Silvestre Silva, Jaime B. Santos, Mario Santos and Alexandra Andre
- 62 **Object tracking with UAVs**
João Palma, Pedro Mendes Jorge and Arnaldo Abrantes
- 63 **Análise da Textura de Padrões Pulmonares em Imagens TCAR Baseada na Lacunaridade**
Verónica Vasconcelos, José Silvestre Silva, Luís Marques and João Barroso
- 69 **Using bioinformatics and biological approaches to uncover novel non-coding disease-related variants**
Patricia Oliveira, Hugo Pinheiro, Sonia Sousa, Joana Carvalho, Karey Shumansky, David Huntsman and Carla Oliveira
- 71 **Voice Type Discovery**
Mário Amado Alves, Ricardo Sousa, Sérgio Lopes, Vítor Almeida and Aníbal Ferreira

Poster Session 3 (15h45 to 16h45)

- 9 **Comparative study of two movement identification strategies on BCI motor task**
Mariana Branco, João Sanches and Rodrigo Ventura
- 10 **EEG time-frequency analysis for ERD/ERS temporal pattern characterization on brain computer interface motor task**
Mariana Branco, Fernando Lopes Da Silva and João Sanches
- 12 **Heart Sound Analysis for Cardiac Pathology Identification: Detection of Systolic Murmurs**
João Pedrosa, Ana Castro and Tiago T. V. Vinhoza
- 16 **Knowledge on Heart Condition of Children based on Demographic and Physiological Features**
Pedro Ferreira, Tiago Vinhoza, Ana Castro, Felipe Mourato, Thiago Tavares, Sandra Mattos, Inês Dutra and Miguel Coimbra
- 18 **Mobile framework for recognition of musical characters**
Rui Silva, Jaime Cardoso and Ana Rebelo
- 27 **SignalBIT Framework: Principles and Applications**
Ana Priscila Alves, Hugo Silva, Andre Lourenco and Ana Fred
- 28 **Correction of Geometrical Distortions in Bands of Chromatography Images**
Bruno Moreira, António Sousa, Ana Maria Mendonça and Aurélio Campilho
- 29 **A novel sparsity and clustering regularization**
Xiangrong Zeng and Mário A. T. Figueiredo
- 30 **Exploiting Two-Dimensional Group Sparsity in 1-Bit Compressive Sensing**
Xiangrong Zeng and Mário A. T. Figueiredo
- 31 **Exploring Heartbeat Sub-patterns for Person Identification**
Carlos Carreiras, Hugo Silva, André Lourenço and Ana Fred
- 32 **Fluorescence Microscopy Based Classification of E-cadherin Missense Mutation Pathogenicity**
Martina Fonseca, Joana Figueiredo, Raquel Seruca and João Sanches
- 40 **A mathematical model of the baroreflex physiology: model parameters measurement**
Anastasiya Strembitska, Alexandre Domingues and João Sanches
- 42 **Automatic sleep parameter computation from Activity and Cardiovascular data**
Alexandre Domingues, João Sanches and Teresa Paiva
- 43 **Supervised Feature Discretization with a Dynamic Bit-Allocation Strategy**
Artur Ferreira and Mario Figueiredo
- 48 **Mosaicing the Interior of Tubular Structures**
David Pereira, João Tomaz, Ricardo Ferreira and José Gaspar

49	On Compression-Based Text Authorship Attribution
	David Pereira Coutinho and Mário A. T. Figueiredo
52	AFM based-force spectroscopy as a functional diagnostic nanotool for hematological diseases
	Filomena Carvalho, Alice Tavares, Mafalda Teodoro, Gabriel Miltenberger-Miltenyi and Nuno Santos
56	Lens Auto-Classification using a Featureless Methodology
	Ricardo Galego, Ricardo Ferreira, Alexandre Bernardino, Etienne Grossmann and José Gaspar
58	Development of amyloid-based biomaterials for nanotechnology
	Gabriela M. Guerra, Sónia Gonçalves, Nuno C. Santos and Ivo C. Martins
60	Autonomous Learning of Tool Affordances
	Afonso Gonçalves, Giovanni Saponaro, Lorenzo Jamone and Alexandre Bernardino
61	Visual Tracking of Buses in a Parking Lot
	Tiago Castanheira, Pedro Silva, Ricardo Ferreira, Alexandre Bernardino and José Gaspar
64	Homing a Teleoperated Car using Monocular SLAM
	Nuno Ribeiro, Ricardo Ferreira and José Gaspar
74	Simultaneous Model Estimation, Denoising, and Noise Decomposition
	Manyá Afonso and João Sanches
75	Webcam Based Optical Tracker for free-hand US
	João André Coelho, David Afonso and João Sanches

Region clustering using colour tuned keypoints

Miguel Farrajota
mafarrajota@ualg.pt
J.M.F. Rodrigues
jrodrig@ualg.pt
J.M.H. du Buf
dubuf@ualg.pt

Vision Laboratory, Inst. for Systems and Robotics,
LARSyS, University of the Algarve
Campus de Gambelas, 8005-139 Faro, Portugal

Abstract

Coloured regions can be segregated by using colour-opponency mechanisms, colour contrast, saturation or luminance. This paper focuses on clustering coloured regions by using colour tuned end-stopped cells. Colour information is coded in separate colour channels to convey differently coloured regions. Then, by using multi-scale cortical end-stopped cells tuned to colour, this information is coded in all channels by mapping it to the multi-scale peaks. Finally, unsupervised clustering is achieved by analysing the branches of these peaks and by linking them together on the basis of their colour, saturation and luminance information.

1 Introduction

Distinguishing visual patches in a scene is important for trying to achieve better and faster object detection and recognition results in computer vision [1]. The development of perceptual grouping algorithms is motivated by the idea that a correct organisation of the visual scene into meaningful regions and/or feature groups will lead to more reliable and efficient methods for object detection, tracking and scene interpretation. These methods are related to two topics of computer vision, namely perceptual organisation and image segmentation. Perceptual organisation deals with the general problem of grouping a set of observed features into meaningful sets [6]. The goal of image segmentation is to decide which parts of the image have a consistent appearance, much like perceptual organisation but in the particular case of grouping pixels according to their similarity [3].

In the human visual system, single- and double-opponent neurons are part of the cortical organisation that extends from area V1 up to the inferotemporal cortex [8]. Single-opponent and double-opponent cells have different functions. Single-opponent cells respond to large coloured regions and inside such regions. Double-opponent cells respond to coloured patterns, textures and colour boundaries. By using retinotopic maps based on such cells, colour, saturation, luminance and spatial information can be combined, which results in tuned clusters of features (keypoints) of image patches. Here, the proposed method is based on labeling keypoints by colour for addressing keypoint clustering.

The major contribution of this paper is the colour segmentation model, without any prior information of the visual scene, but capable of performing well in real-world scenes. We focus on colour information to segment meaningful regions in a uniform colour space (CIE L*C*H). By applying multi-scale cortical end-stopped cells tuned to colour, clustering can be achieved in an unsupervised way and with a high degree of parallelism, while offering robustness to noise and lighting conditions.

2 Colour coding cells and keypoint detection

The method applies a colour gain function in conjunction with a high-pass Butterworth function to the hue channels and a low-pass Butterworth function to the chroma channel for shades, in order to obtain colour- and shade-tuned channels. Here we use the CIE L*C*H* colour space: let image $I(x, y)$, with $N \times M$ pixels, be defined as (L^*, C^*, H^*) .

We divide the hue circle into $N_\phi = 8$ equal ranges (channels). The hue gain functions are Gaussians tuned to specific hues ϕ_j : $\phi_j = j \times 360/N_\phi$ and $j = \{1, 2, 3, \dots, N_\phi\}$. Each hue $H^*(x, y)$ in each channel ϕ_j is weighted by a Gaussian gain function $G_{\phi_j}(x, y) = \exp(-(H_{\phi_j}^*(x, y) - \phi_j)^2/(2\sigma^2))$, with $\sigma = 360/N_\phi$. To the chroma C^* component it is applied a low-pass Butterworth function $BW(x, y) = \sqrt{1/(1 + C^*(x, y)/K)^{2\eta}}$ is applied.

A high-pass BW function is applied to G_{ϕ_j} , which yields the colour contrast $\Psi_{CC_j}(x, y) = G_{\phi_j}(x, y) \times (1 - BW(x, y))$, with $CC_j = \{1, \dots, N_\phi\}$, $\eta = 3$ and $K = 6$. In order to weaken colours with low saturation, a low-pass Butterworth function is applied: $\Psi_{SC}(x, y) = BW(x, y)$ with $K = 8$.

Finally, the luminance is not processed: $\Psi_L = L^*(x, y)$. All colour and shade responses Ψ are normalised between 0 and 1.

The basic principle of multi-scale colour coding is based on Gabor quadrature filters which provide a model of cortical simple cells [7]. In the spatial domain (x, y) they consist of a real cosine and an imaginary sine, both with a Gaussian envelope. Responses of even and odd simple cells, which correspond to real and imaginary parts of a Gabor filter, are obtained by convolving the input image with the filter kernel, and are denoted by $R_{s,i,h}^E(x, y)$ and $R_{s,i,h}^O(x, y)$, being $s = \{8, 12, 16, \dots, \frac{2}{3} \min\{N, M\}\}$ the scales with half-octave increments, the orientations $i = [0, N_\theta - 1]$ with N_θ the number of orientations (here 8), and $h = \{CC_j, SC, L\}$ the colour (CC_j), saturation (SC) and luminance channel (L). Responses of complex cells are modelled by the modulus $C_{s,i,h}(x, y)$ [7] and normalised between 0 and 1.

There are two types of end-stopped cells: single and double [7]. These cells are combined, using $C_{s,i,h}$, in order to obtain the cells' responses in all colour channels. If $[\cdot]^+$ denotes the suppression of negative values, and $C_i = \cos \theta_i$ (with $\theta_i = i\pi/N_\theta$) and $S_i = \sin \theta_i$, then single end-stopped cells are modelled by

$$S_{s,i,h}(x, y) = [C_{s,i,h}(x + dS_{s,i}, y - dC_{s,i}) - C_{s,i,h}(x - dS_{s,i}, y + dC_{s,i})]^+, \quad (1)$$

and double end-stopped ones by

$$D_{s,i,h}(x, y) = \left[C_{s,i,h}(x, y) \times \frac{C_{s,i,h}(x, y) - CS_{s,i,h}(x, y)}{C_{s,i,h}(x, y) + CS_{s,i,h}(x, y)} \right]^+, \quad (2)$$

with $CS_{s,i,h} = \frac{1}{2}C_{s,i,h}(x + 2dS_{s,i}, y - 2dC_{s,i}) + \frac{1}{2}C_{s,i,h}(x - 2dS_{s,i}, y + 2dC_{s,i})$. Distance d is scaled linearly with the filter scale s : $d = 2s$.

Hubel [4] reported some end-stopped cells which did not respond at all to long lines, and he coined them as completely end-stopped cells. Although double end-stopped cells convey information concerning certain patterns, completely end-stopped cells also convey information if the stimulus area is larger than the activation region of the receptive field (RF). Based on such cells, we apply the same property for detecting circular regions. If $CS_{s,i,h}(x, y) > 0.55 \times C_{s,i,h}(x, y)$, then the response of the completely end-stopped cell $CD_{s,i,h}$ is inhibited: $CD_{s,i,h}(x, y) = 0$. If the cell's response is not inhibited, it assumes the same value as the double end-stopped cell: $CD_{s,i,h}(x, y) = D_{s,i,h}(x, y)$.

In this scale space of end-stopped colour cells we look for peaks ("extrema") at each scale which can code differently coloured regions. Cell responses are summed over all orientations: if $\Lambda = \{S, D, CD\}$, then $\hat{\Lambda}_{s,h} = \sum_{i=0}^{N_\theta-1} \Lambda_{s,i,h}/N_\theta$; a threshold $T_i = 0.2$ is applied to inhibit small responses. The maximum responses of all h channels are combined, i.e., $\hat{\Lambda}_s = \max_h \{\hat{\Lambda}_{s,h}\}$, and the local extrema are detected: $E_s^\Lambda = \text{peak}\{\hat{\Lambda}_s\}$ are the peaks of the local maxima of each detected region. Each region in $\hat{\Lambda}_s$ is now assigned a label that corresponds to the ϕ_j of the \max_h , plus two labels for saturation and luminance contrast. The result is an image that has $N_\phi + 2$ labels: $\Gamma(x, y)$ is composed by the maximum colour responses of channels h of $\hat{\Lambda}_s$. This image classifies the keypoints (extrema) with respect to colour.

3 Keypoint clustering

The clustering process consists of four steps: (1) trees of keypoints are clustered in all colour channels in a top-down way; (2) trees which mainly consist of keypoints without (inhibited) completely end-stopped responses are separated from those with such responses – because inhibited responses are due to very elongated regions whereas the other ones are due to circular or semi-circular regions; (3) trees with inhibited completely end-stopped responses within the same hue range ϕ_j are clustered on the

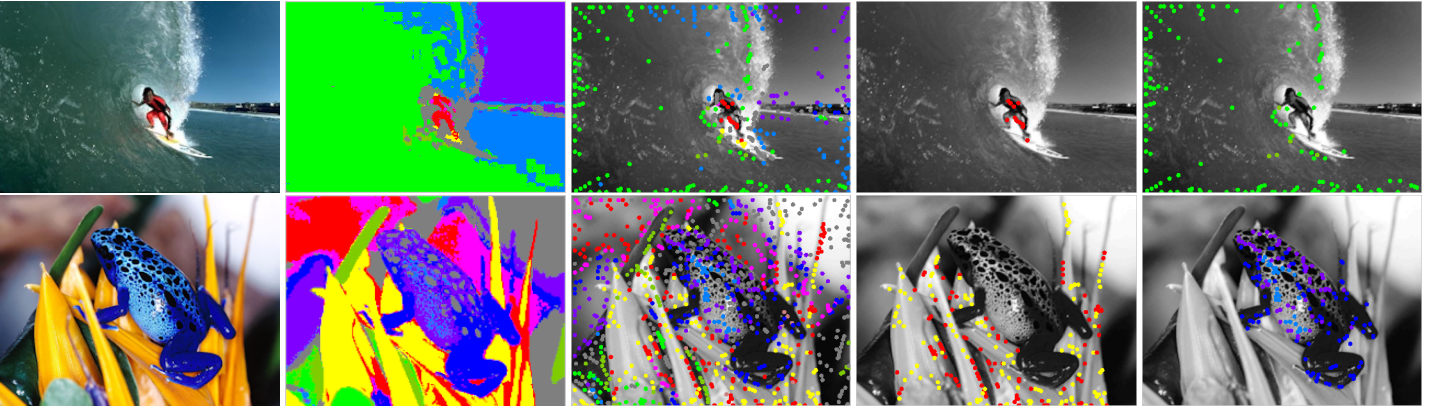


Figure 1: Clustering results of two images: *surfer* (top) and *frog* (bottom). From left to right: input image, maximum colour responses Γ , keypoints, and two examples of clustered patches.

basis of saturation, luminance and spatial continuity; and (4) the resulting clusters are linked to other clusters belonging to neighbouring hue ranges.

Keypoints of the same hue range ϕ and from all scales are combined into trees. We apply a multi-scale tree structure in which one keypoint at a coarse scale is related to one or more keypoints at one finer scale, which can be slightly displaced. This relation is modelled by down-projection using grouping cells with a circular axonic field, the size of which (λ) defines the region of influence; see [2]. Resulting trees mainly composed of responses of completely end-stopped cells are then separated from those with inhibited responses. If a tree *only* comprises keypoints with “completely” responses, then it is considered as a final cluster and it is excluded from further processing.

In the following step, trees of the same colour are clustered with respect to saturation, luminance and spatial continuity. Let T_{A_ϕ} and T_{B_ϕ} be two trees with the same colour. For each tree, the means $\bar{C}_{A_\phi}^* = \sum_1^{N_s} C^*(x, y) / N_s$ and $\bar{L}_{A_\phi}^* = \sum_1^{N_s} L^*(x, y) / N_s$ of the saturation (chroma) and luminance channels are computed, where N_s is the number of scales a particular tree is composed of. If $\bar{C}_{A_\phi}^* > 0.2$ and $\bar{L}_{A_\phi}^* > 0.25$, then the spatial continuity is checked. A binary map B_j is derived from the colour maps CC_j :

$$B_j(x, y) = \begin{cases} 1 & \text{if } CC_j(x, y) \geq 0.7 \\ 0 & \text{if } CC_j(x, y) < 0.7. \end{cases} \quad (3)$$

Now, between two keypoints of each tree, on a straight line connecting both extrema, if $B_j(x, y) = 0$ at 6 or more consecutive pixels, the link is considered invalid until a valid one from all pairs is detected, and the two trees are grouped together. This process is repeated between all trees and clusters of trees until all possible links have been checked.

Finally, clusters of all colours are evaluated and combined in cases where the hue of the underlying patch lies between two hue ranges. The Ψ_{SC} and Ψ_L channels are used in this step. In case of two clusters with neighbouring colours ϕ_l and ϕ_r , with $|l - r| \leq 1$, any two trees from each cluster are compared as in the previous clustering step, where the saturation and luminance means are computed and validated. If positively validated, the minimum distance between the closest two keypoints from both trees is calculated, and if this distance is less than 13 pixels, both clusters are merged. In the case of clusters already composed by two different colour ranges (ϕ_l , ϕ_r), only clusters within the same hue range are considered for validation and merging. As before, this process is repeated until all links have been checked.

4 Discussion and results

This paper presented a biologically inspired method for keypoint detection and clustering. Keypoints labelled by colour provide stable features across images and scales. Also, by exploiting the smoothness of the Gaussian scale space, clustering keypoints into trees constitutes a fairly simple and robust solution for basic grouping of features, with encouraging stability over scales. Likewise, better clustering results can be achieved by using information such as colour continuity, saturation and luminance. More complete and distinct sets of features for coloured regions can be obtained. The usefulness of such a clustering is certainly more focused on object comparison and recognition [5], because groups of features convey better spatial information and this can result in improved matching and more robust results.

Results of the method demonstrate the applicability and usefulness of keypoint grouping. Figure 1 shows results for two images. In the second column, the maximum colour responses Γ show a clear colour sampling and clustering of pixels on the basis of hue. The third column shows all keypoints at all scales, with the same colour coding as in the previous column. Examples of the overall clustering process are illustrated in the right two columns. Shown are the clustered keypoints of the surfer’s wet-suit and the big wave to the left. Also shown are those of the frog and yellow flower, both consisting of two clusters because of two colours.

It can be seen that the results of both images are good but not yet perfect. Although keypoints of the surfer and the greenish wave are correctly clustered, the frog and flower are more difficult. About five keypoints around the frog are not correct. The line of keypoints at the tip of the very thin leaf in the top-right corner (in the fourth column) is missing, but this is likely caused by the different colour, i.e., the very grayish yellow/orange. In general, it is difficult to cluster colours with low saturation levels. Nevertheless, although some details are not perfect, overall results are good enough to be used in matching and segmentation processes.

Acknowledgments

Portuguese Foundation for Science and Technology (FCT) project LARSyS (PEst-OE/EEI/LA0009/2013), project Blavigator RIPD/ADA/109690/2009 and PhD grant to author MF (SFRH/BD/79812/2011).

References

- [1] F. J. Estrada, P. Fua, V. Lepetit, and S. Susstrunk. Appearance-based keypoint clustering. *Computer Vision and Pattern Recognition, 2009. CVPR 2009. IEEE Conference on*, pages 1279–1286, 2009.
- [2] M. Farrajota, J.M.F. Rodrigues, and J.M.H. du Buf. Optical flow by multi-scale annotated keypoints: A biological approach. *Proc. Int. Conf. on Bio-inspired Systems and Signal Processing (BIOSIGNALS 2011), Rome, Italy, 26-29 January*, pages 307–315, 2011.
- [3] Robert M Haralick and Linda G Shapiro. Image segmentation techniques. *Computer vision, graphics, and image processing*, 29(1): 100–132, 1985.
- [4] D. H. Hubel. *Eye, Brain and Vision*, volume 22. Scientific American Library, New York, 1995.
- [5] Gert Kootstra, Jelmer Ypma, and Bart de Boer. Active exploration and keypoint clustering for object recognition. In *Robotics and Automation, 2008. ICRA 2008. IEEE International Conference on*, pages 1005–1010. IEEE, 2008.
- [6] James D McCafferty. *Human and machine vision: computing perceptual organisation*. Ellis Horwood, 1990.
- [7] J. Rodrigues and J.M.H. du Buf. Multi-scale keypoints in V1 and beyond: object segregation, scale selection, saliency maps and face detection. *BioSystems*, 2:75–90, 2006.
- [8] R. Shapley and M. J. Hawken. Color in the cortex: single-and double-opponent cells. *Vision research*, 51(7):701–717, 2011.